CANCER BIOTHERAPY AND RADIOPHARMACEUTICALS
Volume 26, Number 6, 2011

DOI: 10.1089/cbr.2011.1052

Imaging, Autoradiography, and Biodistribution of ^{188}Re-Labeled PEGylated Nanoliposome in Orthotopic Glioma Bearing Rat Model

Feng-Yun J. Huang,[1] Te-Wei Lee,[2] Chih-Hao K. Kao,[3,4] Chih-Hsien Chang,[2] Xiaoning Zhang,[5] Wan-Yu Lee,[1] Wan-Jou Chen,[1] Shu-Chi Wang,[1] and Jem-Mau Lo[1,6]

Abstract

The ^{188}Re-labeled pegylated nanoliposome (abbreviated as ^{188}Re-Liposome) was prepared and evaluated for its potential as a theragnostic agent for glioma. ^{188}Re-BMEDA complex was loaded into the pegylated liposome core with pH 5.5 ammonium sulfate gradient to produce ^{188}Re-Liposome. Orthotopic Fischer344/F98 glioma tumor-bearing rats were prepared and intravenously injected with ^{188}Re-Liposome. Biodistribution, pharmacokinetic study, autoradiography (ARG), histopathology, and nano-SPECT/CT imaging were conducted for the animal model. The result showed that ^{188}Re-Liposome accumulated in the brain tumor of the animal model from 0.28% ± 0.09% injected dose (ID)/g (n = 3) at 1 hour to a maximum of 1.95% ± 0.35% ID/g (n = 3) at 24 hours postinjection. The tumor-to-normal brain uptake ratio (T/N ratio) increased from 3.5 at 1 hour to 32.5 at 24 hours. Both ARG and histopathological images clearly showed corresponding tumor regions with high T/N ratios. Nano-SPECT/CT detected a very clear tumor image from 4 hours till 48 hours. This study reveals the potential of ^{188}Re-Liposome as a theragnostic agent for brain glioma.

Key words: autoradiography, glioma, liposomes, Nano-SPECT/CT, ^{188}Re, theragnostic agent

Introduction

Malignant gliomas, including anaplastic astrocytoma and glioblastma multiforme, are the most common primary central nervous system tumor with high mortality. Conventionally, methods for malignant glioma treatment by surgery and/or radiation therapy have poor prognosis, usually with high recurrence rate and mortality.[1,2] Development of a novel strategy for treatment of malignant gliomas is thus a critical issue.

In the past decade, nanotechnology has been increasingly applied for diagnosis and therapy of cancers, generally using nanoscale particles sized at 20–120 nm. Nanoparticles can be delivered into tumors by the enhanced permeability and retention (EPR) effect[3] and/or by the so called "cellular trojan horse" effect.[4] Liposome, a cell membrane-like phospholipid bilayer structure, is one of the most popular nanoparticles used as carriers for drug delivery. To achieve long circulation in the blood, liposome is generally externally modified with a polyethylene glycol (PEG) group which acts to obstruct the recognition of the liposome by opsonins, thus avoiding uptake by the reticuloendothlial system (RES).[5]

Recently, there have been many radiolabeled liposomes designed for nuclear imaging and/or radiotherapy of cancers including ^{15}O, ^{18}F, ^{64}Cu, ^{67}Ga, ^{90}Y, ^{99m}Tc, ^{111}In, ^{124}I, ^{131}I, ^{177}Lu, ^{186}Re, ^{188}Re, ^{225}Ac etc.[6,7] In 2000, Koukourakis et al.[8] reported a ^{99m}Tc labeled liposome system (i.e., ^{99m}Tc-DTPA-labeled liposome doxorubicin Caelyx®) for detecting glioblastoma.

[1]Department of Biomedical Engineering and Environmental Sciences, National Tsing Hua University, Hsinchu, Taiwan.
[2]Institute of Nuclear Energy Research, Longtan, Taiwan.
[3]Department of Nuclear Medicine, Buddhist Tzu Chi General Hospital, Hualien, Taiwan.
[4]Department of Radiological Technology, Tzu Chi College of Technology, Hualien, Taiwan.
[5]School of Medicine, Tsinghua University, Beijing, China.
[6]Institute of Nuclear Engineering and Science, National Tsing Hua University, Hsinchu, Taiwan.

Address correspondence to: Jem-Mau Lo; Department of Biomedical Engineering and Environmental Sciences, National Tsing Hua University; Kuang-Fu Road, Hsinchu 30013, Taiwan
E-mail: **jmlo@mx.nthu.edu.tw**

^{111}In and ^{18}F labeled liposomes have also been investigated for imaging glioma.[9–11] For radionuclide therapy, ^{188}Re is one of the most attractive radionuclides, decaying with $t_{1/2}$= 16.9 hours by beta emission ($E_{\beta max}$=2.12 MeV) accompanied by gamma emission (E_{γ}=155 keV). This unique property makes ^{188}Re a suitable radionuclide candidate for theragnostic purpose. The high tissue range of emitted beta particles (maximum 11 mm, average 3.8 mm) makes it effective for penetrating solid tumors.[12,13] Moreover, it can be conveniently obtained as a carrier-free species via elution from a ^{188}W/^{188}Re generator.[14]

Bao et al.[15] first proposed a promising avenue for preparation of ^{186}Re/^{188}Re-labeled liposome via encapsulation of ^{186}Re/^{188}Re-*N*,*N*-bis(2-mercaptoethyl) -*N*′,*N*′-diethylethylenediamine (BMEDA) complex in the PEGylated liposome. The ^{186}Re/^{188}Re-labeled liposome has been recently evaluated in the study for cancer therapy using animal models with various tumors such as colon carcinoma ascites,[16–18] colon carcinoma,[19,20] human colorectal adenocarcinoma,[21] ovarian cancer,[22] and head and neck squamous cell carcinoma.[23,24] In these studies, the ^{186}Re/^{188}Re-labeled liposome was employed alone or combining with a chemotherapy drug (e.g., doxorubicin). Moreover, the ^{188}Re-labeled liposome encapsulated with doxorubicin as a bimodal radiochemotherapeutic agent has been recently investigated in a series of translational studies for cancer treatment using animal models with colon cancer and related ascites.[16–21,25]

In this current study, the ^{188}Re-BMEDA complex-encapsulated neutral PEGylated liposomes (abbreviated as ^{188}Re-Liposome) was prepared and evaluated as a diagnostic and therapeutic agent for glioma. An orthotopic glioma tumor-bearing rat model (Fischer/F98) was prepared to mimic the behavior of human malignant astrocytomas for the study.[26,27] Biodistribution, pharmacokinetic study, autoradiography (ARG), whole-body autoradiography (WBARG), histopathology (hematoxylin and eosin [H&E] staining), and nano-SPECT/CT imaging were carried out using this animal model to evaluate the potential of applying ^{188}Re-Liposome as a theragnostic agent for malignant gliomas.

Materials and Methods

Materials

Distearoylphosphatidylcholine (DSPC), cholesterol, and PEG (average molecular weight, 2000)-distearoyl phosphatidylethanolamine (DSPE-PEG_{2000}) were purchased from Genzyme. Cell culture materials and media were from Gibco BRL. PD-10 column and Sepharose 4 Fast Flow were from GE Healthcare. BMEDA was from ABX. H&E staining agents and carboxymethyl cellulose (CMC) were from Sigma-Aldrich. Zoletil® 50 anesthetic was from Virbac (Virbac Taiwan Co., Ltd.). All other chemicals were from Merck.

Cell culture and Fischer/F98 glioma model

F98 glioma cell line (from Dr. Rolf F. Barth, Ohio State University)[26] was cultured in Dulbecco's modified Eagle's medium (containing 10% fetal bovine serum, 100 units/mL penicillin and 100 μM/mL streptomycin). Cells were incubated at 37°C in a humidified environment with 5% CO_2.

All animal studies were approved by the Institutional Animal Care and Use Committee of National Tsing Hua University. The Fischer/F98 orthotopic glioma tumor-bearing rat model was established according to the procedure previously reported by Mathieu et al.[27] with some modifications. The rats (male, 10–11 week old) were anesthetized with isoflurane and then administered atropine sulfate (0.1 mg/kg) via subcutaneous injection before being deep-anesthetized by intraperitoneal injection of Zoletil 50 (15 mg/kg). After anesthesia, the rat head's hair on the operative field was removed and the rats were immobilized by a stereotactic frame. A linear incision was made and the field-open was immobilized for further surgery. After removing the periosteum, a 1-mm diameter hole was made with a high-speed drill at the right brain (located at 3 mm lateral, 5 mm anterior to lambda, and a depth of 5 mm from the skull bone) and the dura carefully pricked with sharp tweezers. For implantation, F98 cells were harvested and re-suspended in Hanks' balanced salt solution (HBBS) plating on ice before use. The 2×10^5 cells in 10 μL HBBS were inoculated into the brain by 27 gauge needle through a nanoliter autoinjector (at the rate of 3 μL/minute). After injection, the needle was retained for 2 minutes and then carefully and slowly withdrawn. Subsequently, paraffin was used to fill the surgical hole and the incision was sutured. The rats were closely observed until complete awakening. On the 12th day after inoculation, the rats implanted with the tumors with the size estimated at 50–100 mm^3 were used for further studies.

Preparation of neutral PEGylated nanoliposome

PEGylated neutral liposome was prepared by the lipid film hydration-extrusion method using repeated freeze-thawing as previously described by Tseng et al.,[28] but with some modifications. Briefly, the mixture of DSPC: cholesterol: DSPE-PEG_{2000} at the molar ratio of 3:2:0.3 was dissolved in chloroform followed by removing the solvent with rotary evaporation. The dry lipid film was rehydrated in 250 mM ammonium sulfate at pH 5.5 and 60°C. After rehydration, liposome was extruded three times through polycarbonate membrane filters with graded pore sizes (0.4, 0.2, 0.1, 0.05, and 0.03 μm) (Costar) via a high-pressure extruder (LIPEXTM; Northern Lipids Inc., Canada). Then the extra-liposomal buffer was changed to normal saline through a Sephadex G-50 column (Pharmacia). Particle size and surface zeta potential of the PEGylated liposome were measured by a dynamic laser scattering analyzer (N4 plus; Beckman Coulter). Phospholipid concentration was measured via phosphate assay[29] with UV-VIS spectrophotometry at λ=830 nm (JascoV-530).

Preparation of ^{188}Re-BMEDA complex and ^{188}Re-Liposome

^{188}Re-BMEDA and ^{188}Re-Liposome were prepared as previously described.[15,16] Rhenium-188 was produced from an alumina-based ^{188}W/^{188}Re generator (Division of Isotope Application, Institute for Nuclear Energy Research).[12,14] ^{188}Re-perrhenate ($Na^{188}ReO_4$) solution was freshly eluted with normal saline from the ^{188}W/^{188}Re generator. The carrier-free ^{188}Re solution was added with BMEDA (5 mg), 0.5 mL of 0.17 M sodium gluconate (in 10% acetate solution), and 120 μL of $SnCl_2$ solution (10 mg/mL). Capped with a rubber septum and aluminum foil, the vial was flushed with N_2 gas before and after addition of 0.5 mL of fresh

^{188}Re-perrhenate (0.37–1.11 GBq). The solution mixture was incubated at 80°C for 1 hour to accomplish ^{188}Re labeling. The radiochemical yield (RCY) of ^{188}Re-BMEDA of the reacted solution was determined by thin layer chromatography (ITLC-SG/normal saline) and the radioactivity was monitored using a TLC scanner (Imaging Scanner System 200; Bioscan).

For ^{188}Re-Liposome preparation, the PEGylated liposome (1 mL) and ^{188}Re-BMEDA (0.37–1.11 GBq) were combined in a vial and capped with a rubber septum and aluminum foil. Then the solution mixture was incubated at 60°C for 30 minutes under shaking at 100 rpm. ^{188}Re-Liposome was separated from the reacted solution using a PD-10 size-exclusion column eluted with normal saline. 0.5-mL fractions were contiguously collected into eppendof tubes. The liposome opacity was visualized to monitor collection of ^{188}Re-Liposome. The radiolabeled yield was determined by the radioactivity of the collected product divided by the total radioactivity of the sample loaded for the separation.

In vitro *stability study*

The stabilities of ^{188}Re-Liposome during incubation in normal saline (at 1:1 volume ratio) at room temperature and rat plasma (at 1:19 volume ratio) at 37°C were studied. At each postincubation time point (1, 4, 24, 48, and 72 hours), a sample of 200 μL was taken and analyzed via a Poly-Prep chromography column (Bio-Red) packed with Sephadex G-50 or Sepharose 4B eluted with normal saline. The radioactivities of the collected fractions were measured by a 2480 WIZARD2TM automatic gamma counter (PerkinElmer). The radiochemical purity (RCP) was determined by the radioactivity of the separated product fractions divided by the total radioactivity of the sample loaded for the separation.

Biodistribution and pharmacokinetic studies

Fifteen orthotopic Fischer344/F98 glioma tumor-bearing rats were used for biodistribution study, randomly divided into five groups, each with 3 rats. After administering ^{188}Re-Liposome (~14.8 MBq) via intravenous injection, rats in each group were sacrificed at different postinjection time points (1, 4, 24, 48, and 72 hours) and the organs and tissues of interest including blood, muscle, testis, pancreas, stomach, small intestine, large intestine, kidney, spleen, liver, lung, heart, normal brain, and brain tumor were dissected, washed, and weighed and the radioactivities were measured using a 2480 WIZARD2TM automatic gamma counter (PerkinElmer). Percentages of injected dose (ID) per gram of the organs or tissues were calculated.

Pharmacokinetic study was conducted according to the reported procedure.[16,30] Six normal adult male Fischer 344 rats (3 rats for each group) were administrated with ^{188}Re-BMEDA (~14.8 MBq) and ^{188}Re-Liposome (~14.8 MBq) via the tail vein. Blood samples (0.3 mL) were collected at 1, 2, 4, 17, 24, 48, and 72 hours postinjection. Radioactivity levels of the blood were expressed as the percentage ID per milliliter. Pharmacokinetic parameters were determined using the WinNonlin software version 5.3. (Pharsight). A noncompartmental analysis model (plasma data, bolus i.v. administration) was used for calculation, following the log/linear trapezoidal rule. The parameters included maximum plasma concentration (C_{max}), total body clearance (Cl), area under the curve (AUC), and mean residence time (MRT).

Ex vivo *ARG and histopathology*

Ex vivo ARG and histopathology studies were performed as previously reported,[24] but with some modification. After 12th day of tumor implantation, the orthotopic Fischer344/F98 glioma tumor-bearing rats were intravenously administered ^{188}Re-Liposome (~44.4 MBq). Then the rats were sacrificed at 1, 4, 24, 48, and 72 hours postinjection and the whole brains were carefully dissected. To embed the dissected brain into an optimal-cutting-temperature (OCT) gel on an oblong plastic holder, the brain and OCT gel were smartly prefrozen in dry ice. The embedded brain sample was placed in a −20°C refrigerator for 1 hour and then transferred to a cryomicrotome (CM3050; Leica) to be ready for slicing. The samples were sliced with 20-μm-thick coronal section by cryomicrotome. For ARG study, these slides were exposed to imaging plates (IPs, BAS-SR2040; Fuji Photo Film) in the cassette (2040; Fuji Photo Film) for 3 days. Subsequently, the IPs were read by using a FLA5100 reader (Fuji Photo Film) with parameters set as reading laser = LD red laser (635 nm), resolution = 25 μm, gradation = 32 bits to acquire the phosphor images. Regions of interest (ROIs) were also circled in tumor, normal brain tissue and background region for use in calculating the intensity of photo-stimulated luminescence (PSL-BG/mm^2) of the tumor and normal brain tissue using Multi Gauge software (version 3.0, Science Lab 2004; Fuji Photo Film). To compare the tumor morphologies between ARG and histopathology images, all samples were cut as back to back slices for ARG and histopathology studies, respectively. In addition, the histopathology study was performed by staining with H&E staining according to a routine stain protocol.

Nano-SPECT/CT imaging and WBARG

Nano-SPECT/CT images were acquired using a nano-SPECT/CT scanner (Bioscan). After 12th day of tumor implantation, the orthotopic Fischer344/F98 glioma tumor-bearing rats were anesthetized with 2% isoflurane and ^{188}Re-Liposome (~300 MBq) was administrated via intravenous injection. Then the rats were positioned prone and imaged at 1, 4, 24, 48, and 72 hours postinjection. The SPECT imaging had multiple pinhole apertures and pyramid collimators, pinhole diameter 2.4 mm, nine pinholes per plate with camera rotation of 360° with four detectors in standard resolution and one circular scan at the start line, one helical scan through the range, one circular scan at the finish line, 20 projections per rotation, 180 seconds per projection, and FOV with helical scanning: 62 × 270 mm. The energy window for SPECT imaging was set at 155% ± 15% keV. The SPECT imaging was immediately followed by CT imaging acquisition with an X-ray source at 45 keV with 0.3 mA and with 512 projections. SPECT was reconstructed by HiSPECT and CT was reconstructed by real-time GPU, and IVS (InvivoScopt) was used for the image fusion.

WBARG was carried out in accordance with the previous procedure.[31] The rat was sacrificed by CO_2 euthanasia after nano-SPECT/CT imaging at 48 hours postinjection and immediately dipped into liquid nitrogen. The frozen carcass

was then embedded in 3% CMC. The frozen CMC block was placed in a refrigerator at −20°C overnight. The sample was attached to the sample stage and sliced with 40-μm-thick transverse section by cryomicrotome (CM 3600; Leica Instruments) at −20°C. Then, the WBARG slides were exposed to IPs in the cassette for 3 days. Subsequently, the IPs were read using a FLA5100 reader with parameter setting as the following: reading laser = LD red laser (635 nm), resolution = 25 μm, gradation = 32 bits. The acquired phosphor images were then analyzed with Multi Gauge software.

Statistical analysis

Data were expressed as mean ± standard deviation. The unpaired t test was used for group comparisons. Values of $p < 0.05$ were considered significant.

Results

Characterization of nanoliposomes and ^{188}Re-Liposomes

Size of the PEGylated liposome was determined to be 80.3 ± 1.1 nm ($n = 3$) and the zeta potential of liposome surface charge was −1.44 mV. The phospholipid concentration of the liposome solution was 21.1 ± 1.7 μmole/mL ($n = 3$). The RCY of ^{188}Re-BMEDA could achieve greater than 98%. The RCY of ^{188}Re-Liposome was 88.0 ± 2.8 ($n = 3$) and the RCP of the purified ^{188}Re-Liposome was 96.0% ± 0.3% ($n = 3$). The liposome after ^{188}Re-BMEDA encapsulation was shown to be of no significant change in size.

In vitro *stability studies*

In vitro stabilities of ^{188}Re-Liposome after incubation in normal saline at room temperature and in rat plasma at 37°C are presented in Figure 1. ^{188}Re-Liposome was stable in normal saline, maintaining a high RCP of 95.56% ± 0.47% ($n = 3$) for at least 72 hours. Stability of ^{188}Re-Liposome slightly declined in plasma, with RCP values of 88.03% ± 2.77% and 74.41% ± 4.80% at 24 and 72 hours ($n = 3$), respectively.

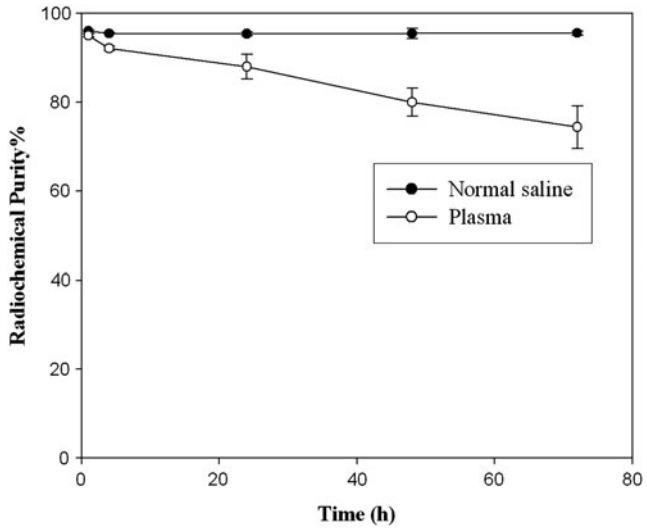

FIG. 1. Stability of ^{188}Re-Liposome in normal saline at room temperature and plasma at 37°C.

Biodistribution studies

Results of biodistribution of ^{188}Re-Liposome in the rats with orthotopic Fischer344/F98 glioma tumor are indicated in Table 1. After intravenous administration, ^{188}Re-Liposome gradually accumulated in brain tumor, reaching a maximum at 1.95% ± 0.35% ID/g at 24 hours postinjection, before starting to decline. In contrast, the accumulation in normal brain was much lower, presented at 0.08% ± 0.02% ID/g at 1 hour postinjection and then progressively decreasing. The tumor-to-normal brain uptake ratio (T/N ratio) increased from 3.5 at 1 hour to 36.3 at 72 hours. The increasing trend of T/N ratios was in compliance with a rising exponential curve (at maximal fitting $R^2 = 0.99$) with a saturated plateau after 24 hours (Fig. 2). Of the organs or tissues, the spleen presented the highest uptake, increasing from 3.50% ± 0.46% ID/g at 1 hour to 29.98% ± 4.19% ID/g at 72 hours. The liver uptake maintained a steady level until 72 hours with the highest value of 2.09% ± 0.45% ID/g at 48 hours. Uptake in the kidneys progressively increased and reached the highest level of 4.65% ± 0.27% ID/g at 72 hours.

Pharmacokinetic studies

The concentration vs. time curves for the clearances of ^{188}Re-BMEDA and ^{188}Re-Liposome from the blood are shown in Figure 3. Pharmacokinetic parameters are summarized in Table 2. From 0 to 72 hours postinjection, the area under the curve ($AUC_{(0\rightarrow 72h)}$) of ^{188}Re-BMEDA and ^{188}Re-Liposome were 10.7 ± 0.2 and 125.8 ± 13.1 hours × % ID/mL, respectively. This result indicated that the $AUC_{(0\rightarrow 72h)}$ of ^{188}Re-Liposome was 12-fold higher than that of ^{188}Re-BMEDA, revealing the long-circulation property of the ^{188}Re-BMEDA encapsulated PEGylated liposome.

Ex vivo *ARG and H&E staining imaging*

Distribution profile of ^{188}Re-Liposome in the brain was studied by the *ex vivo* ARG image and pathological H&E staining image as shown in Figure 4A. Both the ARG and histopathological images clearly showed tumor regions with very high T/N ratios. In addition, the histopathological images indicated a necrotic area in the inner tumor. The semiquantitative ROI analysis from the ARG images revealed that the maximal uptake of ^{188}Re-Liposome in orthotopic Fischer344/F98 glioma tumor reached a maximum uptake (ROI value) at 24 hours postinjection and then progressively declined until 72 hours (Fig. 4B). In contrast to the tumor, uptake in the normal brain was much lower, reaching a maximum value at 1 hour and then progressively decreasing until 72 hours. In semiquantitative analysis of ARG, the T/N ratio was around 5 at 1 hour and rapidly reached a plateau level of around 26 at 24 hours till 72 hours postinjection (Fig. 4B). The increasing trend of T/N ratios was in compliance with a rising exponential curve (at maximal fitting $R^2 = 0.97$) (Fig. 2). As shown in Figure 2, the ARG result was consistent with the biodistribution study.

Nano-SPECT/CT imaging and WBARG

The nano-SPECT/CT imaging of orthotopic Fischer344/F98 glioma tumor-bearing rats that received ^{188}Re-Liposome injection clearly identified the area of tumor lesion (Fig. 5). The maximal accumulation of ^{188}Re-Liposome in the tumor

Table 1. Biodistribution of ^{188}Re-Liposome in Orthotopic Fischer344/F98 Glioma Tumor-Bearing Rats (Mean ± Standard Deviation, $n=3$)

	Uptake (% ID/g)				
Organ	*1 hour*	*4 hours*	*24 hours*	*48 hours*	*72 hours*
Whole blood	5.96 ± 0.95	5.50 ± 0.09	2.01 ± 0.60	1.14 ± 0.13	0.60 ± 0.09
Muscle	0.04 ± 0.01	0.06 ± 0.04	0.05 ± 0.02	0.05 ± 0.02	0.03 ± 0.00
Testis	0.08 ± 0.01	0.11 ± 0.03	0.13 ± 0.01	0.14 ± 0.03	0.14 ± 0.05
Pancreas	0.40 ± 0.00	0.32 ± 0.06	0.28 ± 0.06	0.22 ± 0.09	0.13 ± 0.01
Stomach	0.29 ± 0.05	0.32 ± 0.08	0.36 ± 0.19	0.36 ± 0.21	0.19 ± 0.04
Small intestine	0.43 ± 0.04	0.75 ± 0.24	1.52 ± 0.13	1.16 ± 0.72	1.04 ± 0.31
Large intestine	0.17 ± 0.03	0.14 ± 0.01	0.29 ± 0.05	0.38 ± 0.19	0.30 ± 0.09
Kidney	1.33 ± 0.20	1.58 ± 0.39	2.80 ± 0.83	4.30 ± 0.81	4.65 ± 0.27
Spleen	3.50 ± 0.46	7.44 ± 1.72	19.69 ± 7.80	24.65 ± 4.21	29.98 ± 4.19
Liver	1.78 ± 0.42	1.64 ± 0.11	1.94 ± 0.76	2.09 ± 0.45	1.85 ± 0.24
Lung	1.39 ± 0.20	1.64 ± 0.63	0.71 ± 0.21	0.50 ± 0.10	0.28 ± 0.01
Heart	0.74 ± 0.07	0.63 ± 0.13	0.41 ± 0.06	0.23 ± 0.05	0.15 ± 0.02
Normal brain	0.08 ± 0.02	0.07 ± 0.01	0.06 ± 0.01	0.04 ± 0.02	0.03 ± 0.01
Tumor	0.28 ± 0.09	0.75 ± 0.08	1.95 ± 0.35	1.37 ± 0.39	1.09 ± 0.08
Tumor/normal brain	3.50	10.71	32.50	34.25	36.33

was present at 24 hours after injection, though somewhat shielded with relatively higher background from peripheral brain tissue. The clearest tumor image with the highest T/N ratio was observed at 48 hours postinjection. Figure 6 shows a comparison between the brain images from nano-SPECT/CT and from WBARG. The WBARG image further confirmed the significant accumulation of ^{188}Re-Liposome in the brain tumor lesion and in critical organs (i.e., spleen and liver) at 48 hours postinjection. Enlargement of the brain images from anatomic photogram, autoradiogram, and nano-SPECT/CT clearly shows the corresponding tumor regions (Fig. 6C–E). The whole body autoradiogram image (Fig. 6B) also clearly displays the primary biodistribution of ^{188}Re-Liposome in the rat, including the spleen, kidney, liver, blood (aorta), lung etc. The WBARG autoradiogram is clearly consistent with the anatomical photogram (Fig. 6A). All the imaging results were highly correlated with the biodistribution result (Table 1).

Discussion

Bao et al.[15] reported a technique for loading liposome with the radionuclides, ^{99m}Tc and ^{186}Re/^{188}Re via complexation with BMEDA followed by entrapment in the liposome core with pH 5.5 ammonium sulfate gradient, the so called after-loading method. The lipophilic ^{99m}Tc- or ^{186}/^{188}Re-BMEDA complex is able to cross the lipid bilayer and then become trapped in the liposome core in its protonated form in the acidic gradient. Meanwhile, the after-loading method can also be applied to load doxorubicin into the liposome core.[32] Thus fabrication of ^{186}Re/^{188}Re-labeled liposome can be further combined with loading doxorubicin for the dual

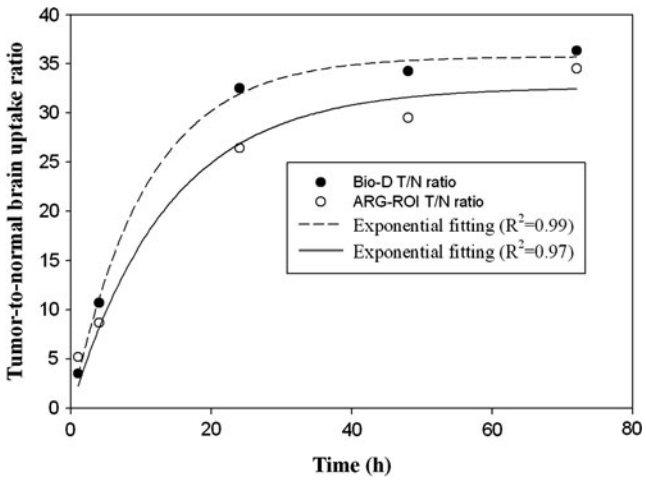

FIG. 2. The curves of tumor-to-normal brain uptake ratio versus postinjection time of ^{188}Re-Liposome obtained from Bio-D and autoradiography (ARG)-region of interest (ROI) studies.

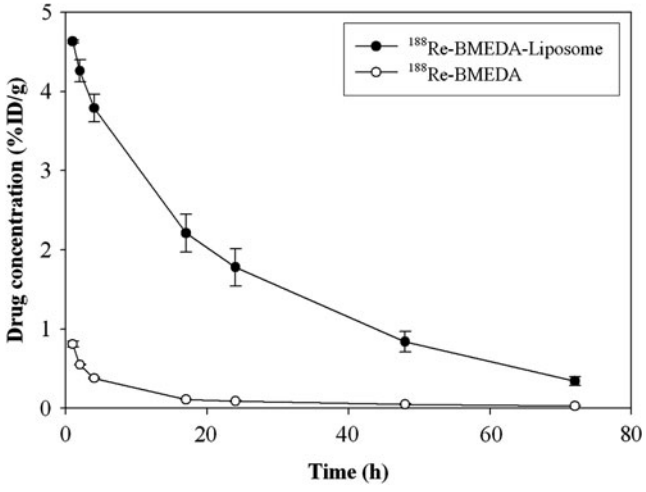

FIG. 3. The curves of concentration of the agent in the blood versus postinjection time of ^{188}Re-*N*,*N*-bis(2-mercaptoethyl) -*N*′,*N*′-diethylethylenediamine (BMEDA) and ^{188}Re-Liposome in normal Fischer344 rats.

Table 2. Pharmacokinetic Parameters of ^{188}Re-BMEDA and ^{188}Re-Liposome Being Intravenously Injected in Normal Fischer344 Rats (% ID/g ± Standard Deviation, $n=3$)

		^{188}Re-BMEDA	*^{188}Re-Liposome*
Parameter	*Unit*	*0–72 hours*	*0–72 hours*
C_{max}	% ID/mL	0.8 ± 0.0	4.6 ± 0.0
Cl	mL/h	9.4 ± 0.2	0.8 ± 0.1[a]
$AUC_{(0\rightarrow\infty)}$	Hours × % ID/mL	10.7 ± 0.2	125.8 ± 13.1[a]
$MRT_{(0\rightarrow\infty)}$	Hours	29.9 ± 0.9	27.1 ± 1.4

[a]$p < 0.05$ (compared with ^{188}Re-BMEDA).

BMEDA, *N,N*-bis(2-mercaptoethyl) -*N′,N′*-diethylethylenediamine; ID, injected dose.

chemo-radionuclide therapy purpose. In this study, ^{188}Re-Liposome was prepared by simply loading ^{188}Re-BMEDA in PEGylated liposome by the after-loading method.

The RCY of ^{188}Re-Liposome could achieve 88.0% ± 2.8%, being comparable to the previous report by a similar method.[15,16] In the stability study, the RCP of ^{188}Re-Liposome in rat plasma was 88.03% ± 2.77% and 74.41% ± 4.80% at 24 and 72 hours postincubation, respectively (Fig. 1). These results were consistent with the previous report by Bao et al.[15] The surface-anchored hydrophilic PEG chains can protect the liposome from the RES uptake and prolong its circulation in the blood. In this current study, the ^{188}Re-labeled liposome with 5.7 mol% PEGylation was prepared. The length of time in circulation for ^{188}Re-Liposome was validated in the pharmacokinetic study (Table 2 and Fig. 3). Clearly, the long-circulating ^{188}Re-Liposome could achieve a clear tumor image, ~2% ID/g and high T/N ratio accumulation in the tumor lesion (Table 1). The density of the designed PEG chains on liposome surface (5.7 mol%) was close to the previously reported 6 mol% PEGylated liposome to minimize RES uptake and probably appropriate for drug delivery for tumor uptake.[33]

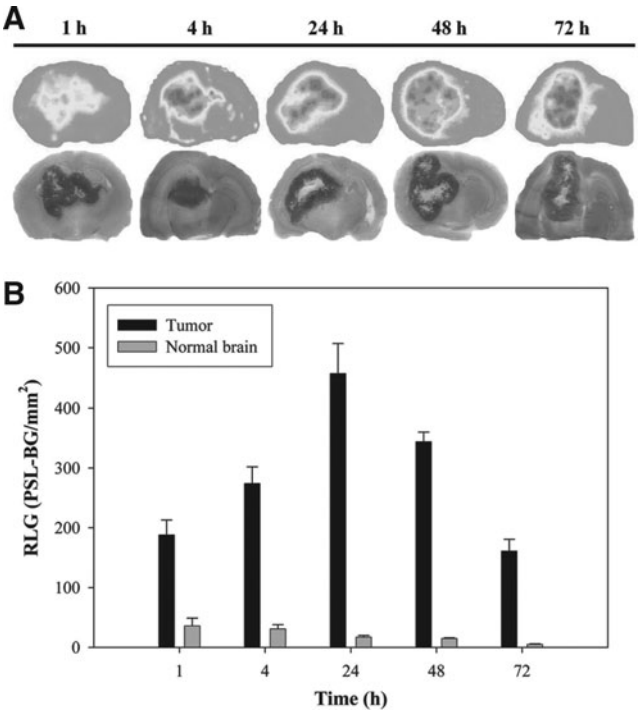

FIG. 4. **(A)** Comparison of ARG and hematoxylin and eosin staining images in the brain of orthotopic Fischer344/F98 glioma tumor-bearing rats after intravenous injection of 37–44.4 MBq of ^{188}Re-Liposome. **(B)** Relative optical intensity photo-stimulated luminescence (PSL-BG/mm^2) of tumor and normal brain derived from autoradiograms images.

Biodistribution results indicated that ^{188}Re-Liposome was rapidly accumulated in the liver and spleen after injection (Table 1). This was due to being recognized by RES of partial ^{188}Re-Liposome from the blood, as previously demonstrated.[34] The main accumulations of ^{188}Re-Liposome were in the liver, spleen, and kidney, with the 72 hours uptake values of 1.85% ± 0.24% ID/g, 29.98% ± 4.19% ID/g, and 4.65% ± 0.27% ID/g, respectively. This result is consistent with the previous work for ^{186}Re-Liposome in a rat model.[15] The biodistribution result was also confirmed with the WBARG study (Fig. 6).

The mechanism for accumulation of ^{188}Re-Liposome in the brain tumor is discussed as follows. First, the glioma usually has the feature of neoangiogenesis, with newly formed vasculatures overpassing BBB properties.[35] At the same time, the glioma cells can act to degrade tight junctions by secreting soluble factors, leading to BBB disruption.[36] Thus, the vasculature-targeting based agent ^{188}Re-Liposome can be allowed to specifically accumulate in glioma. Second, it has been previously reported that the brain tumor endothelial gap size has a modal value of 0.38 μm,[35] making it facile for the neutral liposome accumulation.[37] In this study, ^{188}Re-Liposome sized around 80 nm and with neutral potential (−1.44 mV) could be facilitated to cross the leaky BBB and then significantly accumulate in the tumor lesion by EPR effect. Third, according to the pharmacokinetics of the brain drug delivery proposed by Pardridge,[38] the amount of brain delivery substance may be described as the product of its permeability surface area (PS) and its area under the curve (AUC) at a given time after injection (% ID/g = PS × AUC). Therefore, increasing the AUC of the agent in the blood should improve accumulation of the agent in the brain. In this study, the result of pharmacokinetic analysis showed that the AUC of ^{188}Re-Liposome (125.8 ± 13.1 hours × % ID/mL) was 12-fold higher than ^{188}Re-BMEDA (10.7 ± 0.2 hour × % ID/mL) (Table 2), which could be highly correlated with the improved accumulation of ^{188}Re-Liposome in the brain tumor.

In this study, the results from both biodistribution and semiquantitative ARG showed the highest tumor uptake of ^{188}Re-Liposome to be at 24 hours postinjection (Table 1 and Fig. 4). Further, both biodistribution and ARG T/N ratios (Fig. 2) rapidly reached a plateau at 24 hours and then remained there with a slight increase until 72 hours. The prolongation of maximum uptake from 24 hours to 72 hours could be related to the property of long-circulation of ^{188}Re-Liposome (Table 2). In addition, the phenomenon of the slight increase of T/N ratio after 24 hours could be correlated with the faster washout of ^{188}Re-Liposome from normal brain than from tumor lesion, resulting in the continued slight increase of T/N ratio after 24 hours. This phenomenon could also be validated from the results of nano-SPECT/CT imaging (Fig. 5).

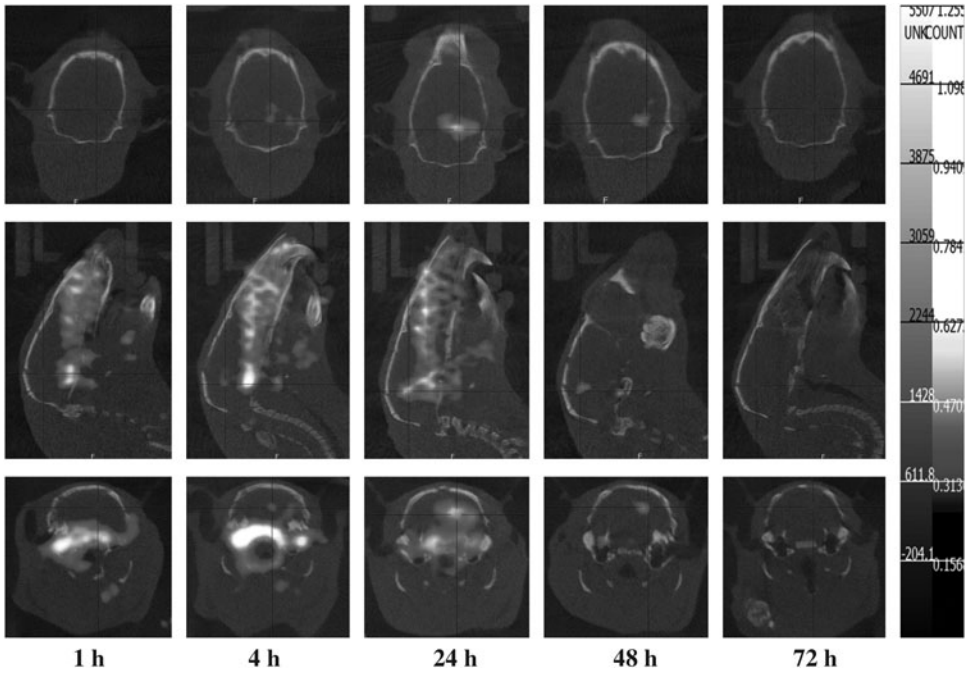

FIG. 5. The dynamic nano-SPECT/CT images of orthotopic Fischer344/F98 glioma tumor-bearing rats along with the period of time after intravenous injection of 296 MBq of ^{188}Re-Liposome.

The nano-SPECT/CT imaging could detect the visible tumor image 4 hours postinjection even though there was just 0.75% ID/g uptake of ^{188}Re-Liposome in the tumor lesion but with a high T/N ratio of 10.71 (Table 1). Nevertheless, the clearest tumor image was present at 48 hours postinjection. This could be due to the different clearance rates of ^{188}Re-Liposome from the tumor and from normal brain tissue, resulting in the continued increase of T/N uptake ratios after 24 hours. The clear tumor image with nano-SPECT/CT for Fischer344/F98 orthotopic glioma bearing rats at 48 hours postinjection could be further confirmed from the result of WBARG (Fig. 6).

Whether the ~2% ID/g accumulation of ^{188}Re-Liposome is high enough for the radiotherapy of brain tumor requires further clarification. The internal radiation dosimetry of critical organs (i.e., liver, spleen, and red marrow) also needs to be considered. To improve the treatment efficacy, a multimodal treatment mode could be introduced to the radiolabeled liposome system. For example, combining chemotherapy drug (e.g., doxorubicin) in ^{188}Re-Liposome as a radiochemotherapeutic liposome agent (^{188}Re-DXR-Liposome) has been evaluated for cancer therapy in a C26 murine colon carcinoma solid tumor model and the results prolonged lifespan of the rats compared with nonchemotherapy drug group (i.e.,^{188}Re-Liposome).[20] Moreover, the active targeting strategy (also called immunoliposome) has the potential to improve the treatment efficacy. In 2005, Mamot et al.[39] reported that using the C225 MAb conjugated immunoliposome (i.e., Anti-EGFR ILs-Dox) could significantly inhibit tumor growth compared with nontargeted liposome (Lipo-Dox/PLD) in a human glioma mouse model. This significant results and strategy could be highly correlated with epidermal growth factor receptor (EGFR/HER1/ErbB1) overexpression occurring in 40% of gliomas.[40]

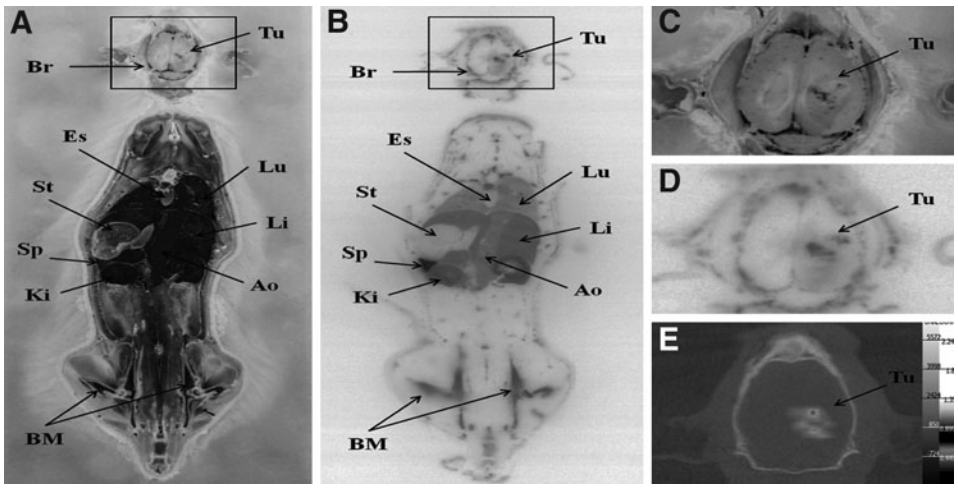

FIG. 6. Comparison of transverse whole body ARG brain image with local brain image of nano-SPECT/CT in orthotopic Fischer344/F98 glioma tumor-bearing rats. The anatomic photography **(A)** and ARG **(B)** were performed following local brain nano-SPECT/CT imaging. The enlarged anatomic photogram **(C)** and enlarged autoradiogram **(D)** of the brain are compared with nano-SPECT/CT image of the brain **(E)**. Br, brain; Tu, tumor; Es, esophagus; St, stoma; Sp, spleen; Ki, kidney; Lu, lung; Li, liver; Ao, Aorta; BM, bone marrow.

Conclusions

The imaging, ARG and biodistribution studies of the long-circulating ^{188}Re-Liposome on orthotopic Fischer344/F98 glioma tumor-bearing rat model demonstrated a very high T/N ratio and clear tumor scintigraphic image. This study is significant in paving the way for further development of ^{188}Re-Liposome as a theragnostic agent for treating brain glioma. The active targeting strategy and therapeutic efficacy of ^{188}Re-Liposome on the glioma animal model will be further studied in our future research.

Acknowledgments

We sincerely thank all the group members of the Radiopharmacology Laboratory of Institute of Nuclear Energy Research (INER), Longtan, Taiwan, for technical assistance and meaningful discussion and also Dr. Tsai-Yueh Luo and Mr. Ching-Jun Liu of the Division of Isotope Application of INER for providing rhenium-188 for the study. This study was funded by a grant (No. 992001INER075) from the INER and by a Bilateral Tsing Hua Collaborative Project (No. 99N2447E1) from the National Tsing Hua University, Hsinchu, Taiwan.

Disclosure Statement

No competing financial interests exist.

References

1. Raizer JJ. HER1/EGFR tyrosine kinase inhibitors for the treatment of glioblastoma multiforme. J Neurooncol 2005; 74:77.
2. Reardon DA, Rich JN, Friedman HS, et al. Recent advances in the treatment of malignant astrocytoma. J Clin Oncol 2006;24:1253.
3. Maeda H, Wu J, Sawa T, et al. Tumor vascular permeability and the EPR effect in macromolecular therapeutics: A review. J Control Release 2000;65:271.
4. Choi MR, Stanton-Maxey KJ, Stanley JK, et al. A cellular Trojan horse for delivery of therapeutic nanoparticles into tumors. Nano Lett 2007;7:3759.
5. Torchilin VP. Recent advances with liposomes as pharmaceutical carriers. Nat Rev Drug Discov 2005;4:145.
6. Phillips WT, Goins BA, Bao A. Radioactive liposomes. Wires Nanomed Nanobi 2009;1:69.
7. Ting G, Chang CH, Wang HE, et al. Nanotargeted radionuclides for cancer nuclear imaging and internal radiotherapy. J Biomed Biotechnol 2010; DOI: 10.1155/2010/953537.
8. Koukourakis MI, Koukouraki S, Fezoulidis I, et al. High intratumoural accumulation of stealth (R) liposomal doxorubicin (Caelyx (R)) in glioblastomas and in metastatic brain tumours. Br J Cancer 2000;83:1281.
9. Harrington KJ, Mohammadtaghi S, Uster PS, et al. Effective targeting of solid tumors in patients with locally advanced cancers by radiolabeled pegylated liposomes. Clin Cancer Res 2001;7:243.
10. Khalifa A, Dodds D, Rampling R, et al. Liposomal distribution in malignant glioma: Possibilities for therapy. Nucl Med Commun 1997;18:17.
11. Oku N, Yamashita M, Katayama Y, et al. PET imaging of brain cancer with positron emitter-labeled liposomes. Int J Pharm 2011;403:170.
12. Hsieh BT, Lin WY, Luo TY, et al. Production of carrier-free Re-188 in the past ten years in Taiwan. J Radioanal Nucl Ch 2007;274:569.
13. Huang FY, Huang LK, Lin WY, et al. Development of a thermosensitive hydrogel system for local delivery of Re-188 colloid drugs. Appl Radiat Isotopes 2009;67:1405.
14. Knapp FF, Callahan AP, Beets AL, et al. Processing of reactor-produced W-188 for fabrication of clinical-scale alumina-based W-188/Re-188 generators. Appl Radiat Isotopes 1994;45:1123.
15. Bao A, Goins B, Klipper R, et al. Re-186-liposome labeling using Re-186-SNS/S complexes: *In vitro* stability, imaging, and biodistribution in rats. J Nucl Med 2003;44:1992.
16. Chen LC, Chang CH, Yu CY, et al. Biodistribution, pharmacokinetics and imaging of Re-188-BMEDA-labeled pegylated liposomes after intraperitoneal injection in a C26 colon carcinoma ascites mouse model. Nucl Med Biol 2007;34:415.
17. Chen LC, Chang CH, Yu CY, et al. Pharmacokinetics, micro-SPECT/CT imaging and therapeutic efficacy of Re-188-DXR-liposome in C26 colon carcinoma ascites mice model. Nucl Med Biol 2008;35:883.
18. Chang CH, Stabin MG, Chang YJ, et al. Comparative dosimetric evaluation of nanotargeted Re-188-(DXR)-liposome for internal radiotherapy. Cancer Biother Radiopharm 2008;23:749.
19. Chang YJ, Chang CH, Chang TJ, et al. Biodistribution, pharmacokinetics and microSPECT/CT imaging of Re-188-BMEDA-liposome in a C26 murine colon carcinoma solid tumor animal model. Anticancer Res 2007;27:2217.
20. Chang YJ, Chang CH, Yu CY, et al. Therapeutic efficacy and microSPECT/CT imaging of Re-188-DXR-liposome in a C26 murine colon carcinoma solid tumor model. Nucl Med Biol 2010;37:95.
21. Chen MH, Chang CH, Chang YJ, et al. MicroSPECT/CT imaging and pharmacokinetics of Re-188-(DXR)-liposome in human colorectal adenocarcinoma-bearing mice. Anticancer Res 2010;30:65.
22. Zavaleta CL, Goins BA, Bao A, et al. Imaging of Re-186-liposome therapy in ovarian cancer xenograft model of peritoneal carcinomatosis. J Drug Target 2008;16:626.
23. Wang SX, Bao A, Herrera SJ, et al. Intraoperative Re-186-liposome radionuclide therapy in a head and neck squamous cell carcinoma xenograft positive surgical margin model. Clin Cancer Res 2008;14:3975.
24. Soundararajan A, Bao A, Phillips WT, et al. [Re-186]Liposomal doxorubicin (Doxil): *In vitro* stability, pharmacokinetics, imaging and biodistribution in a head and neck squamous cell carcinoma xenograft model. Nucl Med Biol 2009;36:515.
25. Liu CM, Chang CH, Chang YJ, et al. Preliminary evaluation of acute toxicity of Re-188-BMEDA-liposome in rats. J Appl Toxicol 2010;30:680.
26. Barth RF, Kaur B. Rat brain tumor models in experimental neuro-oncology: The C6, 9L, T9, RG2, F98, BT4C, RT-2 and CNS-1 gliomas. J Neurooncol 2009;94:299.
27. Mathieu D, Lecomte R, Tsanaclis AM, et al. Standardization and detailed characterization of the syngeneic Fischer/F98 glioma model. Can J Neurol Sci 2007;34:296.
28. Tseng YL, Hong RL, Tao MH, et al. Sterically stabilized anti-idiotype immunoliposomes improve the therapeutic efficacy of doxorubicin in a murine B-cell lymphoma model. Int J Cancer 1999;80:723.
29. Bartlett GR. Phosphorus assay in column chromatography. J Biol Chem 1959;234:466.

30. Li SD, Chen YC, Hackett MJ, et al. Tumor-targeted delivery of siRNA by self-assembled nanoparticles. Mol Ther 2008;16:163.
31. Lee WC, Hwang JJ, Tseng YL, et al. Therapeutic efficacy evaluation of (111)in-VNB-liposome on human colorectal adenocarcinoma HT-29/luc mouse xenografts. Nucl Instrum Meth A 2006;569:497.
32. Barenholz Y. Liposome application: Problems and prospects. Curr Opin Colloid Interface Sci 2001;6:66.
33. Chow TH, Lin YY, Hwang JJ, et al. Therapeutic efficacy evaluation of In-111-labeled PEGylated liposomal vinorelbine in murine colon carcinoma with multimodalities of molecular imaging. J Nucl Med 2009;50:2073.
34. Poste G, Bucana C, Raz A, et al. Analysis of the fate of systemically administered liposomes and implications for their use in drug delivery. Cancer Res 1982;42:1412.
35. Kemper EM, Boogerd W, Thuis I, et al. Modulation of the blood-brain barrier in oncology: Therapeutic opportunities for the treatment of brain tumours? Cancer Treat Rev 2004;30:415.
36. Schneider SW, Ludwig T, Tatenhorst L, et al. Glioblastoma cells release factors that disrupt blood-brain barrier features. Acta Neuropathol 2004;107:272.
37. Ogihara I, Kojima S, Jay M. Differential uptake of Gallium-67-labeled liposomes between tumors and inflammatory lesions in rats. J Nucl Med 1986;27:1300.
38. Pardridge WM. Non-invasive drug delivery to the human brain using endogenous blood-brain barrier transport systems. Pharm Sci Technol To 1999;2:49.
39. Mamot C, Drummond DC, Noble CO, et al. Epidermal growth factor receptor-targeted immunoliposomes significantly enhance the efficacy of multiple anticancer drugs *in vivo*. Cancer Res 2005;65:11631.
40. Yarden Y, Sliwkowski MX. Untangling the ErbB signalling network. Nat Rev Mol Cell Biol 2001;2:127.